

Spatial Entanglement in Decaying Biparticle Systems

M. V. Fedorov^{1,*}, M. A. Efremov¹, A. E. Kazakov¹, K. W. Chan², C. K. Law³, and J. H. Eberly²

¹A. M. Prokhorov General Physics Institute, Russian Academy of Sciences, Vavilova str., 38, Moscow, 119991 Russia

²Center for Quantum Information and Department of Physics and Astronomy, University of Rochester, Rochester, NY, 14627 USA

³Department of Physics, The Chinese University of Hong Kong, NT, Hong Kong SAR, China

*e-mail: fedorov@ran.gpi.ru

Received December 27, 2004

Abstract—The electron and ion wavepackets arising via the photoionization process and spontaneous emission of a photon by an atom are investigated theoretically in three dimensions with the initial wavefunction of a finite-mass atom taken in the form of a finite-size wavepacket. Recoil and wavepacket spreading are completely taken into account. Both the total photoelectron–ion and atom–photon wavefunctions are found in the coordinate representations as a solution of the initial-value problem. Entanglement arising in the electron photoionization and spontaneous emission processes is shown to be closely related to the structure of particle wavepackets, which can be measured in the coincidence and single-particle schemes of measurements. In particular, the two main specific predicted effects arising under the conditions of high entanglement are anomalous narrowing of the coincidence wavepackets and, under different conditions, anomalous broadening of the single-particle wavepackets.

1. INTRODUCTION

Theoretical description of photoionization and spontaneous emission of an atom is usually based on the crucial assumptions concerning the infinitely large mass of an atom and the absolutely well-defined position of its nucleus [1–4]. Obviously, neither of these two assumptions is rigorously true. In contrast, we assume here that both the mass of an atom and the localization size of its center-of-mass wavefunction are finite (as is assumed also in [5–7]). Such a formulation of the problems gives rise to many new interesting questions related to entanglement of electron–ion quantum states, the structure of particle wavepackets, etc. These are the problems addressed in this report.

The electron–ion entanglement and wavepacket structure have been described in our recent work [7]. This topic and the derived results are given a brief overview in Section 3. In Section 4, we consider spontaneous emission of a photon and discuss atom–photon entanglement, as well as the atomic and photon wavepacket structures. Common features of these two phenomena and some differences between them will be described. These considerations are preceded by Section 2, where we give a series of general definitions of the parameters characterizing entanglement and wavepacket structure.

2. DEFINITIONS

By definition, entanglement is equivalent to nonfactorization. If a two-particle wavefunction $\Psi(x_1, x_2)$ cannot be presented in the form of a product of two single-particle functions

$$\Psi(x_1, x_2) \neq \psi_1(x_1)\psi_2(x_2), \quad (1)$$

this can be considered as direct indication that quantum states of the system under consideration are entangled. In Eq. (1), x_1 and x_2 are arbitrary variables or sets of variables of particles 1 and 2.

There are several ways to characterize the degree and conditions of entanglement. One of the most appropriate is characterization by the so-called Schmidt number K [6, 8, 9], which is defined as the inverse trace of the squared reduced density matrices

$$K = [\text{Tr}_1(\rho_{r1}^2)]^{-1} = [\text{Tr}_2(\rho_{r1}^2)]^{-1}, \quad (2)$$

where $\rho_{r1,2} = \text{Tr}_{1,2}(\rho)$ and $\rho = |\Psi\rangle\langle\Psi|$. The entanglement is large if $K > 1$, and there is no entanglement if $K = 1$.

For investigation of manifestations of entanglement in wavepacket structures, one can use a comparison of wavepacket widths to be found from single-particle and coincidence schemes of measurements, $\Delta x_{1,2}^{(s)}$ and $\Delta x_{1,2}^{(c)}$. The parameter R , characterizing the degree of entanglement that can be seen in such a measurement scheme, is defined as the ratio of these widths [7]:

$$R = \frac{\Delta x_{1,2}^{(s)}}{\Delta x_{1,2}^{(c)}}. \quad (3)$$

In the nonentangled states, $R \equiv 1$. If there is some degree of entanglement, the parameter R can either coincide with or differ from the Schmidt number K . The difference can arise owing to spreading of wavepackets in the coordinate representation.

3. PHOTOIONIZATION

Let an atom be ionized by a laser pulse, the intensity and pulse duration of which are such that the total ionization per pulse is complete but there is still no ATI. A characteristic time of ionization is estimated as $1/\gamma_i$, where γ_i is the ionization rate according to Fermi's Golden Rule. We will consider times much longer than $1/\gamma_i$. The time immediately after ionization will be referred to as the initial time $t = 0$.

As is well known [10], in the dipole approximation, the variables in the Schrödinger equation for an atom in a laser field can be separated if one takes them as the relative-motion and center-of-mass variables \mathbf{r}_{rel} and \mathbf{r}_{cm} :

$$\mathbf{r}_{\text{rel}} = \mathbf{r}_e - \mathbf{r}_i, \quad \mathbf{r}_{\text{cm}} = \frac{m_e \mathbf{r}_e + m_i \mathbf{r}_i}{M}, \quad (4)$$

where \mathbf{r}_e and \mathbf{r}_i are the electron and ion position vectors. Owing to this, the total two-particle wavefunction both during and after ionization has the form

$$\Psi(\mathbf{r}_e, \mathbf{r}_i, t) = \Psi_{\text{cm}}(\mathbf{r}_{\text{cm}}, t) \Psi_{\text{rel}}(\mathbf{r}_{\text{rel}}, t). \quad (5)$$

As the variables \mathbf{r}_{rel} and \mathbf{r}_{cm} (Eq. (4)) do not coincide with \mathbf{r}_e and \mathbf{r}_i , in the last pair of really observable variables wavefunction (5) is not factorized, and this is the reason for entanglement.

Let us assume that, initially, the atomic center-of-mass wavefunction $\Psi_{\text{cm}}(\mathbf{r}_{\text{cm}}, t)$ is prepared in the form of a Gaussian wavepacket with a width $\Delta r_{\text{cm}}^{(0)}$ and, then, it is left to spread freely:

$$|\Psi_{\text{cm}}(\mathbf{r}_{\text{cm}}, t)|^2 = \frac{1}{[\sqrt{2\pi}\Delta r_{\text{cm}}(t)]^3} \exp\left(-\frac{\mathbf{r}_{\text{cm}}^2}{2[\Delta r_{\text{cm}}(t)]^2}\right), \quad (6)$$

where $\Delta r_{\text{cm}}(t)$ is the time-dependent width of the center-of-mass wavepacket

$$\Delta r_{\text{cm}}(t) = \left\{ [\Delta r_{\text{cm}}^{(0)}]^2 + \left(\frac{\hbar t}{2M\Delta r_{\text{cm}}^{(0)}}\right)^2 \right\}^{1/2} \approx \begin{cases} \Delta r_{\text{cm}}^{(0)}, & t \ll t_{\text{spr}}^{(\text{cm})}, \\ v_{\text{spr}}^{(\text{cm})} t, & t \gg t_{\text{spr}}^{(\text{cm})}, \end{cases} \quad (7)$$

$t_{\text{spr}}^{(\text{cm})} = 2M[\Delta r_{\text{cm}}^{(0)}]^2/\hbar$ is its spreading time, and M is the total mass of an atom.

As for the relative-motion wavefunction $\Psi_{\text{rel}}(\mathbf{r}_{\text{rel}}, t)$ after ionization, it can be found rather easily in the Weisskopf–Wigner approximation [7], giving

$$|\Psi_{\text{rel}}(\mathbf{r}_{\text{rel}}, t)|^2 = \frac{3 \cos^2 \theta_{\text{rel}}}{16\pi r_{\text{rel}}^2 \Delta r_{\text{rel}}^{(0)}} \times \exp\left(\frac{r_{\text{rel}} - vt}{\Delta r_{\text{rel}}^{(0)}}\right) \left| 1 - \text{Erf}\left[\frac{i}{\sqrt{2}}\left(\frac{\sqrt{\zeta}}{2} - \frac{i}{\sqrt{\zeta}} \frac{r_{\text{rel}} - vt}{\Delta r_{\text{rel}}^{(0)}}\right)\right]\right|^2, \quad (8)$$

where Erf is the error function, θ_{rel} is the angle between \mathbf{r}_{rel} and the polarization vector of the ionizing laser field, $\Delta r_{\text{rel}}^{(0)} = v/2\gamma_i$ is the initial width of the relative-motion wavepacket, $v = \sqrt{2\mu E_{\text{kin}}}$ and E_{kin} are its mean velocity and kinetic energy, $\zeta = t/t_{\text{spr}}^{(\text{rel})}$, μ is the reduced mass, and $t_{\text{spr}}^{(\text{rel})}$ is the spreading time for the relative motion

$$t_{\text{spr}}^{(\text{rel})} = \frac{\mu[\Delta r_{\text{rel}}^{(0)}]^2}{\hbar}. \quad (9)$$

Equation (8) describes a spherical wavepacket in r_{rel} with an angular modulation determined by the factor $\cos^2 \theta_{\text{rel}}$, propagating in the direction of growing r_{rel} with velocity v . At times shorter than $t_{\text{spr}}^{(\text{rel})}$, the wavepacket $|\Psi_{\text{rel}}|^2$ has a sharp edge at $r_{\text{rel}} = vt$ and an exponentially falling tail at $r_{\text{rel}} < vt$:

$$|\Psi_{\text{rel}}(\mathbf{r}_{\text{rel}}, t)|^2 = \frac{3 \cos^2 \theta_{\text{rel}}}{4\pi \Delta r_{\text{rel}}^{(0)} r_{\text{rel}}^2} \exp\left(\frac{r_{\text{rel}} - vt}{\Delta r_{\text{rel}}^{(0)}}\right) \theta(vt - r_{\text{rel}}), \quad (10)$$

where the radial width of the wavepacket is equal to $\Delta r_{\text{rel}}^{(0)} = v/2\gamma_i$. In the large-spreading regime, $t \gg t_{\text{spr}}^{(\text{rel})}$, $|\Psi_{\text{rel}}|^2$ (8) takes the Lorentzian shape:

$$|\Psi_{\text{rel}}(\mathbf{r}_{\text{rel}}, t)|^2 = \frac{3 \cos^2 \theta_{\text{rel}}}{8\pi^2 r_{\text{rel}}^2} \frac{\Delta r_{\text{rel}}(t)}{(r_{\text{rel}} - vt)^2 + [\Delta r_{\text{rel}}(t)]^2/4}, \quad (11)$$

where $\Delta r_{\text{rel}}(t)$ is the long-time limit of the time-dependent radial width of the relative-motion wavepacket

$$\Delta r_{\text{rel}}(t) = \begin{cases} \Delta r_{\text{rel}}^{(0)} = \frac{v}{2\gamma_i}, & t \ll t_{\text{spr}}^{(\text{rel})} \quad (\zeta \ll 1) \\ v_{\text{spr}}^{(\text{rel})} t = 2\frac{\hbar\gamma_i}{\mu v} t, & t \gg t_{\text{spr}}^{(\text{rel})} \quad (\zeta \gg 1) \end{cases} \approx \Delta r_{\text{rel}}^{(0)} \sqrt{1 + \left(\frac{t}{t_{\text{spr}}^{(\text{rel})}}\right)^2}. \quad (12)$$

The widths $\Delta r_{\text{cm}}(t)$ (Eq. (7)) and $\Delta r_{\text{rel}}(t)$ (Eq. (12)) can be combined into a single control parameter:

$$\eta(t) = \frac{\Delta r_{\text{cm}}(t)}{\Delta r_{\text{rel}}(t)} \approx \frac{\Delta r_{\text{cm}}^{(0)}}{\sqrt{2}\gamma_i} \sqrt{\frac{1 + (t/t_{\text{spr}}^{(\text{cm})})^2}{1 + (t/t_{\text{spr}}^{(\text{rel})})^2}}. \quad (13)$$

The dependences on this parameter accumulate in themselves both the dependences on the initial conditions and on the time after ionization t .

Equations (5), (6), and (8) can be used for finding the widths of the electron and atomic wavepackets to be measured in the coincidence and single-particle measurement schemes; e.g., for a photoelectron, the results are given by

$$\begin{aligned} \Delta r_e^{(c)}(t) &\approx \min \left\{ \frac{M}{m_e} \Delta r_{\text{cm}}(t), \Delta r_{\text{rel}}(t) \right\} \\ &\approx \Delta r_{\text{rel}}(t) \frac{\eta(t)}{\sqrt{\eta^2(t) + m_e^2/M^2}}, \end{aligned} \quad (14)$$

$$\begin{aligned} \Delta r_e^{(s)}(t) &\approx \max \left\{ \Delta r_{\text{cm}}(t), \frac{m_i}{M} \Delta r_{\text{rel}}(t) \right\} \\ &\approx \Delta r_{\text{rel}}(t) \sqrt{\eta^2(t) + m_i^2/M^2}. \end{aligned}$$

A ‘‘natural’’ width of the electron wavepacket is $\Delta r_{\text{rel}}(t)$. This is the width that can be found in the approximations of an infinitely heavy atom ($M \rightarrow \infty$) and infinitely narrow center-of-mass wavepacket ($\Delta r_{\text{cm}}(t) \rightarrow 0$). Deviations of $\Delta r_e^{(c)}(t)$ and $\Delta r_e^{(s)}(t)$ from $\Delta r_{\text{rel}}(t)$ occur in the regions of very small and large values of the control parameter $\eta(t)$ (Eq. (13)): $\Delta r_e^{(c)}(t)$ is anomalously small ($\ll \Delta r_{\text{rel}}(t)$) at $\eta(t) \ll m_e/M$ and $\Delta r_e^{(s)}(t)$ is anomalously large ($\gg \Delta r_{\text{rel}}(t)$) at $\eta(t) \gg 1$. Both of these two effects can be characterized by the condition of large values of the parameter $R(t)$ (Eq. (3)). The dependence of $R(t)$ on the control parameter $\eta(t)$ (Eq. (13)) is shown in Fig. 1. The initial values of $R(t)$ are indicated by dots, and they can be shown to coincide with the Schmidt number $K(1)$, $R(0) = K$. The directions of the time evolution of the parameter $R(t)$ are indicated by arrows. These directions depend on the position of $R(0)$ on the $\eta(t)$ axis with respect to the point $\eta_* = \sqrt{m_e/m_i}$. Asymptotic values of $R(t)$ at $t \rightarrow \infty$ coincide with $R(0)$. If $K \gg 1$, the entanglement is large, and it remains constant at all times t , because, after ionization, the particles practically do not interact with each other. The region where, in this case, $R(t) \approx 1$ can be interpreted as the hidden-entanglement region, where entanglement does not manifest itself in the coordinate wavepacket structures. The second curve shown in Fig. 1 corresponds to photodissociation of a molecule decaying into two equal-mass fragments. In this case, the hidden-entanglement

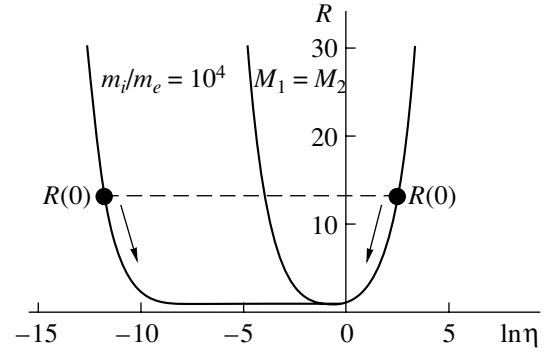


Fig. 1. Plot of the entanglement parameter $R(3)$ as a function of $\eta(t)$ (13) for the photoionization process.

region is seen to degenerate into a single point. This means that, in the case of molecular photodissociation with almost any initial conditions, the difference between the coincidence and single-particle wavepackets is well-pronounced.

4. SPONTANEOUS EMISSION

By assuming that, initially (at $t = 0$), an atom is excited to some level E_e and then the emission of a photon begins, let us present the time-dependent atom-photon vector of state in the form

$$\begin{aligned} |\Psi(t)\rangle &= \sum_{\mathbf{q}} C_{\mathbf{q}}(t) |e\rangle |\mathbf{q}\rangle |0\rangle \exp\left(-\frac{i}{\hbar} \left(\frac{q^2}{2M} + E_e\right) t\right) \\ &+ \sum_{\mathbf{q}, \mathbf{k}\lambda} C_{\mathbf{q}, \mathbf{k}\lambda}(t) |g\rangle |\mathbf{q}\rangle |1_{\mathbf{k}\lambda}\rangle \exp\left(-\frac{i}{\hbar} \left(\frac{q^2}{2M} + E_g + \hbar\omega_{\mathbf{k}}\right) t\right), \end{aligned} \quad (15)$$

where $C_{\mathbf{q}}$ and $C_{\mathbf{q}, \mathbf{k}\lambda}$ are the expansion coefficients, $|e\rangle$ and $|g\rangle$ refer to the excited and ground atomic states, \mathbf{q} is the momentum of the atomic center of mass, $|0\rangle$ and $|1_{\mathbf{k}\lambda}\rangle$ denote the vacuum and one-photon state vectors of the field, and \mathbf{k} and λ are the photon wavevector and polarization index. After emission (at $\gamma t \gg 1$), the first term on the right-hand side of Eq. (15) vanishes and the coefficients $C_{\mathbf{q}, \mathbf{k}\lambda}(t)$, calculated in the Weisskopf–Wigner approximation, take the form [5]

$$\begin{aligned} &C_{\mathbf{q}, \mathbf{k}\lambda}(t) \Big|_{\gamma t \gg 1} \\ &= -i \frac{\omega_0 \sqrt{2\pi}}{L^{3/2} \sqrt{\hbar\omega_{\mathbf{k}}}} \frac{(\mathbf{d}_{eg} \cdot \mathbf{e}_{\lambda})}{\sqrt{\mathbf{q}^2 - (\mathbf{q} + \hbar\mathbf{k})^2} + \omega_{\mathbf{k}} - \omega_0 + i\frac{\gamma}{2}} C_{\mathbf{q} + \hbar\mathbf{k}}^{(0)}, \end{aligned} \quad (16)$$

where $\mathbf{d}_{eg} = \langle e | \mathbf{d} | g \rangle$ is the dipole matrix element and γ is the total decay rate. The initial position- and momentum-dependent atomic center-of-mass wavepackets

$\Psi_{\text{cm}}^{(0)}(\mathbf{r}_{\text{at}}, t=0)$ and $C_{\mathbf{q}}^{(0)}$ are taken below in the Gaussian form

$$\Psi_{\text{cm}}^{(0)}(\mathbf{r}_{\text{at}}, t=0) = \frac{1}{(\sqrt{\pi}\Delta r_{\text{at}}^{(0)})^{3/2}} \exp\left(-\frac{\mathbf{r}_{\text{at}}^2}{2[\Delta r_{\text{at}}^{(0)}]^2}\right),$$

$$C_{\mathbf{q}}^{(0)} = \left(\frac{2\hbar\sqrt{\pi}}{L\Delta q_0}\right)^{3/2} \exp\left(-\frac{\mathbf{q}^2}{2\Delta q_0^2}\right),$$
(17)

with the initial sizes of the atomic coordinate and momentum wavepackets equal to $\Delta r_{\text{at}}^{(0)}$ and $\Delta q_0 = \hbar/\Delta r_{\text{at}}^{(0)}$.

The function $C_{\mathbf{q}, \mathbf{k}\lambda}(t)|_{\gamma \gg 1}$ (Eq. (16)) has the meaning of the entangled two-particle atom–photon wavefunction in the momentum representation. Its Schmidt-mode analysis was given in [6]. Below, we present an alternative approach based on the calculation and analysis of the position- and time-dependent atom–photon wavefunction [3, 11]

$$\Psi(\mathbf{r}_{\text{at}}, \mathbf{r}_{\text{ph}}, t) = \frac{1}{L^3} \sum_{\mathbf{q}, \mathbf{k}\lambda} \mathbf{e}_\lambda C_{\mathbf{q}, \mathbf{k}\lambda}$$

$$\times \exp\left\{\frac{i}{\hbar}\left[\mathbf{q}\mathbf{r}_{\text{at}} + \hbar\mathbf{k}\mathbf{r}_{\text{ph}} - \left(\frac{q^2}{2M} + E_g + \hbar\omega_{\mathbf{k}}\right)t\right]\right\}.$$
(18)

Not dwelling upon the details of calculations, let us reproduce the final result of integration over \mathbf{q} and \mathbf{k} :

$$|\Psi(\mathbf{r}_{\text{at}}, \mathbf{r}_{\text{ph}}, t)|^2$$

$$= \left|\Psi_{\text{at}}\left(\mathbf{r}_{\text{at}} + \frac{v_{\text{rec}}}{c}(\mathbf{r}_{\text{ph}} - \mathbf{r}_{\text{at}}), t\right)\right|^2 |\Psi_{\text{ph}}(\mathbf{r}_{\text{ph}} - \mathbf{r}_{\text{at}}, t)|^2,$$
(19)

where $v_{\text{rec}} = \hbar\omega_0/Mc$ is the atomic recoil and Ψ_{at} and Ψ_{ph} are the entanglement-free atomic and photon wavefunctions:

$$|\Psi_{\text{at}}(\mathbf{r}_{\text{at}}, t)|^2 = \frac{1}{[\sqrt{\pi}\Delta r_{\text{at}}(t)]^3} \exp\left(-\frac{\mathbf{r}_{\text{at}}^2}{[\Delta r_{\text{at}}(t)]^2}\right),$$

$$|\Psi_{\text{ph}}(\mathbf{r}_{\text{ph}}, t)|^2$$

$$= \frac{3}{8\pi\Delta r_{\text{ph}}^2} \frac{\sin^2\theta_{\mathbf{r}}}{\mathbf{r}_{\text{ph}}^2} \exp\left(\frac{|\mathbf{r}_{\text{ph}}| - ct}{\Delta r_{\text{ph}}}\right) \theta(ct - |\mathbf{r}_{\text{ph}}|),$$
(20)

where $\theta_{\mathbf{r}}$ is the angle between \mathbf{r}_{ph} and \mathbf{e}_0 , \mathbf{e}_0 is the unit vector along the polarization of the field exciting the atom, $\Delta r_{\text{ph}} = c/\gamma$ is the time-independent width of the

photon wavepacket, and $\Delta r_{\text{at}}(t)$ is the time-dependent width of the spreading atomic wavepacket:

$$\Delta r_{\text{at}}(t) = \left\{[\Delta r_{\text{at}}^{(0)}]^2 + \left(\frac{\hbar t}{M\Delta r_{\text{at}}^{(0)}}\right)^2\right\}^{1/2}. \quad (21)$$

Equation (20) can be interpreted as the center-of-mass atomic wavefunction for a nonemitting atom in its ground state and the wavefunction of a photon emitted by an infinitely heavy atom with a delta-localized center-of-mass wavefunction. However, in the situation under consideration, the atom is initially excited and its mass and localization size are finite. For these reasons, the arguments of the atomic and photon protofunctions \mathbf{r}_{at} and \mathbf{r}_{ph} in product (19) are entangled. This is why two-particle wavefunction (19) does not factorized in the variables \mathbf{r}_{at} and \mathbf{r}_{ph} and there is some degree of entanglement. It is important to notice that expression (19) is very similar to Eq. (5) occurring for photoionization. The latter turns into Eq. (19) with the help of the substitution $m_e/m_i \rightarrow v_{\text{rec}}/c$. With this substitution, many results of the previous section appear to be valid for spontaneous emission too. In particular, in an analogy with Eq. (13), we can introduce the control parameter

$$\eta(t) = \frac{\Delta r_{\text{at}}(t)}{c/\gamma} \approx \frac{\gamma\Delta r_{\text{at}}^{(0)}}{c} \left\{1 + \left(\frac{\hbar t}{M[\Delta r_{\text{at}}^{(0)}]^2}\right)^2\right\}^{1/2}. \quad (22)$$

Furthermore, similarly to the derivation of Eq. (14), we can find atomic and photon wavepacket widths that can be measured in the coincidence and single-particle scheme:

$$\Delta r_{\text{ph}}^{(c)}(t) \approx \min\left\{\frac{c}{v_{\text{rec}}}\Delta r_{\text{at}}(t), \frac{c}{\gamma}\right\} \approx \frac{c}{\gamma} \frac{\eta(t)}{\sqrt{\eta^2(t) + v_{\text{rec}}^2/c^2}},$$

$$\Delta r_{\text{ph}}^{(s)}(t) \approx \max\left\{\Delta r_{\text{at}}(t), \frac{c}{\gamma}\right\} \approx \frac{c}{\gamma} \sqrt{\eta^2(t) + 1}$$
(23)

and

$$\Delta r_{\text{at}}^{(c)}(t) \approx \min\left\{\Delta r_{\text{at}}(t), \frac{c}{\gamma}\right\} \approx \Delta r_{\text{at}}(t) \frac{1}{\sqrt{\eta^2(t) + 1}},$$

$$\Delta r_{\text{ph}}^{(s)}(t) \approx \max\left\{\Delta r_{\text{at}}(t), \frac{v_{\text{rec}}}{\gamma}\right\}$$

$$\approx \Delta r_{\text{at}}(t) \frac{\sqrt{\eta^2(t) + v_{\text{rec}}^2/c^2}}{\eta(t)}.$$
(24)

Coefficients c/γ and Δr_{at} in front of the dependences on η in Eqs. (23) and (24) can be considered as natural widths of photon and atomic entanglement-free protofunctions (20). Deviations from these natural widths

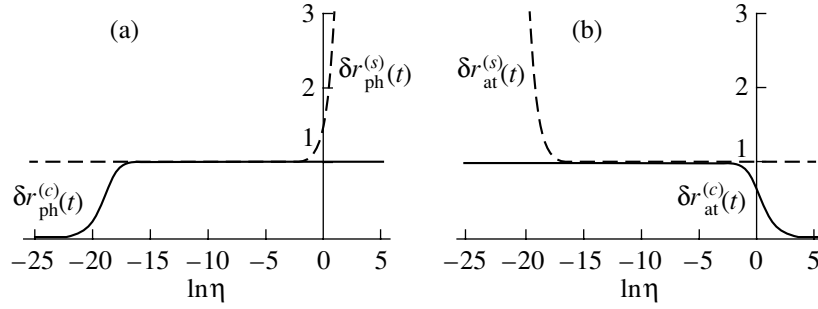


Fig. 2. Relative width of the photon (a) and atomic (b) coordinate wavepackets.

are related to the manifestations of entanglement in the wavepacket structures. To show conditions under which such deviations can occur, the relative widths $\delta r_{ph}^{(c),(s)}(t) = (\gamma/c)\Delta r_{ph}^{(c),(s)}(t)$ and $\delta r_{at}^{(c),(s)}(t) = \Delta r_{at}^{(c),(s)}(t)/\Delta r_{at}(t)$ are plotted in Fig. 2 in their dependence on the control parameter η . These pictures show clearly that deviations from the natural widths can occur only in the regions of small and large values of η . For example, the coincidence width of the photon wavepacket experiences anomalous narrowing at $\eta < v_{rec}/c$. Let us discuss the physical explanation of this effect. According to the Heisenberg uncertainty relation, the size $\Delta r_{at}(t)$ of the atomic wavefunction corresponds to the velocity uncertainty of the atomic center of mass, $\Delta v = \hbar/M\Delta r_{at}$. Owing to the Doppler effect, this gives rise to broadening of the spectrum of emitted photons up to the width $\delta\omega = k\Delta v = \hbar\omega_0/Mc\Delta r_{at} = v_{rec}/\Delta r_{at}$. At $\eta(t) < v_{rec}/c$, this broadening $\delta\omega$ exceeds the natural spectral width of the emitted light $\Delta\omega = \gamma$, $\delta\omega = (v_{rec}/c\eta)\Delta\omega > \Delta\omega$, which has been noticed in [6]. Since the photons of all frequencies are emitted coherently, integration over ω in the interval $\delta\omega$ shortens the effective emission time and spatial size of the emitted photon wavepacket to $t_{eff} = 1/\delta\omega = \Delta r_{at}/v_{rec}$ and $\Delta r_{ph} = ct_{eff} = (c/\gamma)(c\eta/v_{rec})$, which are much smaller than $1/\gamma$ and c/γ , respectively, if $\eta(t) \ll v_{rec}/c$.

In the opposite case of large values of the control parameter, $\eta(t) > 1$, Fig. 2a shows that the *single-particle width* of the photon wavepacket appears to be much larger than the natural width c/γ . Qualitatively, this effect of *anomalously large entanglement-induced broadening* of the photon single-particle wavepacket is explained by the spatially coherent inhomogeneous broadening. If the atomic wavepacket is very wide, $\Delta r_{at}(t) > c/\gamma$ (or $\eta(t) > 1$), relatively short (narrow, $\Delta r_{ph} = c/\gamma$) photon wavepackets can be emitted from any point inside the atomic wavepacket. All such contributions are summed coherently to form an integral photon wavepacket of width determined by the atomic wavepacket size, i.e., by $\Delta r_{at}(t)$. It should be noted that the initial stage of the photon wavepacket broadening, occurring when $\Delta r_{at}(t) \ll c/\gamma$, was described in [12],

where a sharp θ -function front wing of the photon outgoing wave was shown to smooth slightly.

Moreover, by comparing Eqs. (23) and (24), we find that the relative atomic and photon widths obey the following reciprocity relations:

$$\delta r_{ph}^{(c)}(t)\delta r_{at}^{(s)}(t) = \delta r_{ph}^{(s)}(t)\delta r_{at}^{(c)}(t) = 1. \quad (25)$$

Finally, in a direct analogy with the case of photoionization, we can introduce the parameter R determined as the ratio of the single-particle $\Delta r^{(s)}$ to coincidence $\Delta r^{(c)}$ widths of the particles' wavepackets. For spontaneous emission, this parameter is given by

$$R(t) = \frac{\Delta r_{ph}^{(s)}}{\Delta r_{ph}^{(c)}} = \frac{\Delta r_{at}^{(s)}}{\Delta r_{at}^{(c)}} \quad (26)$$

$$= \sqrt{1 + \eta^2(t)} \sqrt{1 + \frac{1}{\eta^2(t)} \left(\frac{v_{rec}}{c}\right)^2}.$$

The dependence of $R(t)$ on the control parameter $\eta(t)$ (Eq. (22)) is shown in Fig. 3. The parameter $R(t)$ is large at small ($\eta(t) \ll 1$) and large ($\eta(t) \gg 1$) values of the control parameter $\eta(t)$, i.e., just where the above-described *entanglement-induced narrowing or broadening* of wavepackets occurs. At intermediate values of $\eta(t)$, $R(t) \approx 1$. The time evolution of the parameter $R(t)$ is related to spreading of the atomic center-of-mass

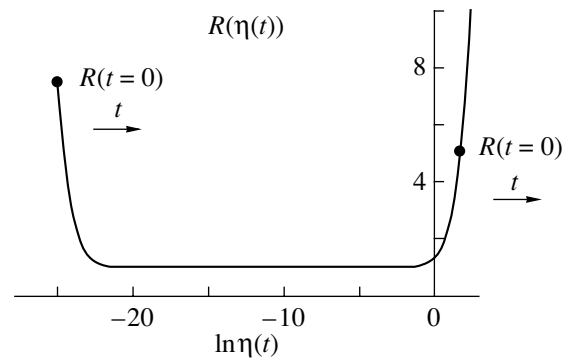


Fig. 3. The parameter R (26) vs. the control parameter $\eta(t)$ (22).

wavepacket $\Delta r_{\text{at}}(t)$. Owing to spreading, $\Delta r_{\text{at}}(t)$ (Eq. (21)) and $\eta(t)$ (Eq. (22)) are always growing functions of time t . For this reason, the direction of the time evolution of $R(t)$ in Fig. 3 is always to the right (as shown by arrows) independent of the initial conditions, which is different from the case of photoionization. The second difference between spontaneous emission and photoionization concerns the limiting value of $R(\eta(t))$ at $t \rightarrow \infty$. In the case of photoionization, $\eta(t \rightarrow \infty)$ is finite and $R(t \rightarrow \infty) = R(t = 0)$ [7]. In the case of spontaneous emission, the parameter $R(\eta(t))$ grows unboundedly: $R(\eta(t)) \rightarrow \infty$ at $t \rightarrow \infty$. These rather strongly pronounced differences show that there is no complete identity between the cases of two massive particles and a massive plus a massless one.

5. CONCLUSIONS

To summarize, we have evaluated the space-time behavior of the joint quantum state arising in two processes: (a) atom photoionization and (b) spontaneous emission by an atom. In these cases, the finite mass of the atom and the finite initial size of its center-of-mass wavefunction are taken into account. The relationship between the wavepacket structures of particles (atom and photoelectron, emitted photon and atom) and entanglement in the decaying atomic systems is analyzed. We have indicated how entanglement can be identified experimentally and quantitatively. First, the two specific (entanglement-induced) discovered effects are anomalous narrowing and anomalous broadening of the coordinate atomic and photon wavepackets to be observed in the coincidence and single-particle measurement schemes. Second, we introduced the entanglement parameter R , the ratio between the entanglement-free wavepacket width and the coincidence wavepacket width. We gave expressions for R in terms of ionization (decay) rate and packet spreading velocity (or initial wavepacket widths) that are, of course, themselves determined by underlying atomic parameters. It was shown that R depends in a simple way on the basic

control parameter $\eta(t)$ and can be much larger than unity at small and large values of $\eta(t)$. The conditions for experimental observation of the described effects are discussed.

ACKNOWLEDGMENTS

The research reported here has been supported by the National Science Foundation (USA, grant no. PHY-0072359), the Hong Kong Research Grants Council (grant no. CUHK4016/03P), the Russian Foundation for Basic Research (grant nos. 02-02-16400 and 05-02-16469), the Russian Science Support Foundation (MAE), and the award of a Messersmith Fellowship (K.W.C.).

REFERENCES

1. V. Weisskopf and E. Wigner, *Z. Phys.* **63**, 54 (1930).
2. M. O. Scully and M. S. Zubairy, *Quantum Optics* (Cambridge Univ. Press, Cambridge, 1997).
3. L. Mandel and E. Wolf, *Optical Coherence and Quantum Optics* (Cambridge Univ. Press, Cambridge, 1995).
4. M. V. Fedorov, *Atomic and Free Electrons in a Strong Light Field* (World Sci., Singapore, 1997).
5. K. Rzazewski and W. Zakowicz, *J. Phys. B* **25**, L319 (1992).
6. K. W. Chan, C. K. Law, and J. H. Eberly, *Phys. Rev. Lett.* **88**, 100402 (2002); *Phys. Rev. A* **68**, 022110 (2003).
7. M. V. Fedorov, *et al.*, *Phys. Rev. A* **69**, 052117 (2004).
8. M. A. Nielsen and I. L. Chuang, *Quantum Computation and Quantum Information* (Cambridge Univ. Press, Cambridge, 2000).
9. A. Ekert and P. L. Knight, *Am. J. Phys.* **63**, 415 (1995).
10. L. D. Landau and E. M. Lifshitz, *Quantum Mechanics: Non-Relativistic Theory* (Nauka, Moscow, 1989; Pergamon Press, Oxford, 1977).
11. W. P. Schleich, *Quantum Optics in Phase Space* (Wiley, New York, 2001).
12. O. Steuernagel and H. Paul, *Phys. Rev. A* **53**, 2983 (1996).